Accurate modeling of electron-hole binding in CuCl. II. Biexciton wavefunction

Junko Usukura [1,2] Selvakumar V. Nair [3] and Eiji Tokunaga [2]

[1] *Institute for Solid State Physics, University of Tokyo, 5-1-5 Kashiwanoha, Kashiwa, Chiba 277-8581, Japan*

[2] *Department of Physics, Tokyo University of Science, 1-3 Kagurazaka, Shinjuku-ku, Tokyo 162-8601, Japan*

[3] *Centre for Advanced Nanotechnology, University of Toronto, 170 College Street, Toronto, Ontario M5S 3E3, Canada*

(Received 29 December 2019; revised 5 June 2020; accepted 15 July 2020; published 5 August 2020)

We present an approach to calculate the biexciton ground state including the electron-longitudinal-optical-phonon coupling and an accurate variational function to describe the Coulomb correlations in the biexciton. We apply this method to the long-standing problem of biexciton binding energy in CuCl and obtain a binding energy of 32.6 meV. We also discuss the effect of electron-hole (*e*-h) exchange interaction on the biexciton binding energy. Including correction due to *e*-h exchange, the theoretical binding energy is 28.8 meV, in good agreement with the experimental value of 32 meV. Details of the biexciton wavefunction are presented in the form of correlation functions with respect to two-particle separations, which show how the particles in the biexciton are distributed.

DOI: 10.1103/PhysRevB.102.075203

I. INTRODUCTION

In ionic semiconductors charged particles strongly interact with longitudinal optical (LO) phonons. An electron moving slowly in a polar crystal can be pictured as a polaron, a quasiparticle consisting of an electron accompanied by a cloud of phonons. Effects resulting from this coupling to phonons emerge even in optical processes related to excitons and biexcitons. In this paper we develop a method to calculate the biexciton ground state including electron- and hole-phonon couplings and Coulomb correlations using a variational approach.

Our approach is based on a method of decoupling electronic and phononic degrees of freedom developed by Haken [1] for an exciton interacting with phonons. In this method the exciton-phonon coupled state is described as a product of a purely electronic wavefunction and a coherent state for the phonon cloud dressing the electron-hole pair. The phonon displacement describing the coherent state can be variationally determined along with the electronic wavefunction. The binding energies of the exciton in the Rydberg states [2,3] as well as the lowest state [4,5] in various polar semiconductors have been obtained by a variational method with ansatz for the phonon displacement function proposed by Pollmann and Büttner (PB) [6].

Several authors have attempted to model the biexciton state coupled to phonons. Schmidt [7] discussed an effective potential including the effect of the lattice vibration on the biexciton. However, that calculation was based on crude assumptions such as neglecting the momenta of excitons and assuming equal electron and hole masses ($m_e/m_h = 1$). Pollmann and Büttner [8] calculated the biexciton binding energy using the the Heitler-London approximation for the electronic wavefunction, which makes their calculation limited to $m_e/m_h \sim 0$. In the absence of electron-phonon coupling, accurate variational calculations using a correlated Gaussian basis have been performed [9] but the calculated binding energy in CuCl, for example, is underestimated by 25% compared to the experimental value. We showed in Ref. [10] that, because of LO-phonon coupling, the exciton binding energy cannot be interpreted as the Coulomb Rydberg and a reanalysis of the biexciton problem using an approach that accurately includes both the Coulomb interaction and LO-phonon coupling is required.

Another weakness of previous studies on the biexciton was an incomplete decoupling of the center-of-mass motion which makes it difficult to use general variational forms for the wavefunction. We completely eliminate the center-of-mass motion using a unitary transformation which allows us to generalize the PB method to the biexciton problem without making an approximation on the electron-hole mass ratio. In most semiconductors the effective hole mass is larger than the effective electron mass, but it is not large enough to neglect the motion of the hole. Hence the biexciton is more like the positronium molecule, which is a system consisting of two electrons and two positrons, rather than the helium molecule in which the protons are much heavier than the electrons. In analogy with the positronium molecule [11], we represent the electronic wavefunction as a sum of correlated Gaussians to flexibly express pair correlations between particles in a general way.

The success of this approach is demonstrated by comparison with experiments. As a first application, here we consider CuCl, which has a long history of experimental and theoretical studies on excitons and biexcitons [12–19]. The valence-band structure of CuCl is rather simple: The valence band related to creation of the biexciton is a single hole band ($j = 1/2$ spin-orbit split-off band), unlike most cubic semiconductors that require a more elaborate treatment of the hole due to the fourfold degeneracy of the heavy-hole and light-hole bands.

The rest of the paper is organized as follows. In Sec. II we formulate the theoretical approach for describing the biexciton-phonon system. Using a variational ground-state wavefunction that includes the translational motion and the

phonon coherent state we derive an effective Hamiltonian for the biexciton. We then describe the use of the correlated Gaussian basis set to variationally solve for the ground state of this effective Hamiltonian. In Sec. III we present the results for CuCl, which includes the biexciton energy as well as the biexciton wavefunction, which is presented in the form of two-particle correlation functions. In Sec. IV we estimate the correction to the binding energy due to the electron-hole exchange interaction. Finally we discuss our results and present our conclusions in Sec. V.

II. THEORETICAL FORMALISM

A. Effective potential

We first introduce the approach to the exciton-phonon system and then describe how it can be extended to the biexciton-phonon system. The Hamiltonian describing an electron-hole pair interacting via statically screened Coulomb interaction and dynamically coupled to LO phonons by Fröhlich interaction is given by

$$H_x = \frac{\hat{\boldsymbol{P}}_x^2}{2M_x} + \frac{\hat{\boldsymbol{p}}^2}{2\mu} - \frac{e^2}{\varepsilon_\infty r} + \sum_{\boldsymbol{k}} \hbar\omega_0 a_{\boldsymbol{k}}^\dagger a_{\boldsymbol{k}} + \sum_{\boldsymbol{k}} [V_k a_{\boldsymbol{k}} \rho_{\boldsymbol{k}}(\boldsymbol{r}) e^{i\boldsymbol{k}\cdot\boldsymbol{R}_x} + \text{H.c.}], \tag{1}$$

with

$$V_k = -\frac{i}{k}\sqrt{\frac{2\pi e^2 \hbar\omega_0}{V\varepsilon^*}}, \quad \frac{1}{\varepsilon^*} = \frac{1}{\varepsilon_\infty} - \frac{1}{\varepsilon_0}, \tag{2}$$

$$\rho_{\boldsymbol{k}}(\boldsymbol{r}) = e^{is_h\boldsymbol{k}\cdot\boldsymbol{r}} - e^{-is_e\boldsymbol{k}\cdot\boldsymbol{r}}, \tag{3}$$

where $\boldsymbol{R}_x$ and $\boldsymbol{r}$ are, respectively, the center-of-mass and relative coordinates of the exciton; ε_0 and ε_∞ are, respectively, the static and optical dielectric constants; $M_x = m_e + m_h$ is the exciton mass; μ is the exciton reduced mass; $s_e = m_e/M_x$; and $s_h = m_h/M_x$. Here m_e (m_h) denotes the effective mass of the electron (hole).

Motivated by the Lee-Low-Pines transformation for the electron polaron [20], Haken assumed a product-state form for the wavefunction of the exciton-phonon system [1] as

$$|\Psi_x\rangle = T_x U_x \psi_x(\boldsymbol{r})|0\rangle, \tag{4}$$

where

$$T_x = \exp\left[i\left(\boldsymbol{Q}_x - \sum_{\boldsymbol{k}} \boldsymbol{k} a_{\boldsymbol{k}}^\dagger a_{\boldsymbol{k}}\right)\cdot\boldsymbol{R}_x\right] \tag{5}$$

is the well-known translation operator that decouples the center-of-mass motion with the total momentum, $\boldsymbol{Q}_x$, of the coupled system. Here the subscript "x" indicates that the symbols are relevant to the exciton-phonon system and distinct from those for the biexciton-phonon system appearing in Eq. (10). The phonon state $U_x|0\rangle$ is assumed to be the coherent state generated by the displacement operator

$$U_x(\boldsymbol{r}) = \exp\left[\sum_{\boldsymbol{k}} \{F_{\boldsymbol{k}}^*(\boldsymbol{r}) a_{\boldsymbol{k}} - F_{\boldsymbol{k}}(\boldsymbol{r}) a_{\boldsymbol{k}}^\dagger\}\right], \tag{6}$$

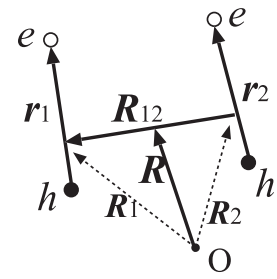

FIG. 1. Coordinates representing the 2e-2h system. $\boldsymbol{r}_i = \boldsymbol{r}_{ei} - \boldsymbol{r}_{hi}$ is the relative coordinate for the ith exciton X_i ($i = 1, 2$), $\boldsymbol{R}_{12}$ is the relative coordinate between the two excitons, and $\boldsymbol{R}$ is the center of mass.

where $|0\rangle$ is the phonon vacuum state. As discussed in Ref. [10] it is possible to calculate, quite generally, the exciton wavefunction $\psi_x(\boldsymbol{r})$ and phonon displacement amplitudes $F_k(\boldsymbol{r})$ that minimize total energy. However, such a treatment is not easily extended to the biexciton system. We therefore consider the Pollmann-Büttner ansatz [6] for $F_k(\boldsymbol{r})$,

$$F_{\boldsymbol{k}}(\boldsymbol{r}) = v_k^*\left(f_{\boldsymbol{k}}^h e^{-is_e\boldsymbol{k}\cdot\boldsymbol{r}} - f_{\boldsymbol{k}}^e e^{is_h\boldsymbol{k}\cdot\boldsymbol{r}}\right), \tag{7}$$

where $v_k = V_k/\hbar\omega_0$, and $f_{\boldsymbol{k}}^e$ and $f_{\boldsymbol{k}}^h$ are determined variationally.

Now, we turn to the biexciton-phonon system. The two-electron–two-hole (2e-2h) system can be conveniently described in relative coordinates, $\boldsymbol{r}_1$, $\boldsymbol{r}_2$, and $\boldsymbol{R}_{12}$, and the center of mass, $\boldsymbol{R}$, as shown in Fig. 1. The conjugate momenta of $\boldsymbol{r}_1$, $\boldsymbol{r}_2$, $\boldsymbol{R}_{12}$, and $\boldsymbol{R}$ are denoted by $\hat{\boldsymbol{p}}_1$, $\hat{\boldsymbol{p}}_2$, $\hat{\boldsymbol{P}}_{12}$, and $\hat{\boldsymbol{P}}$, respectively. The Hamiltonian describing the biexciton coupled to phonons is given by

$$H_{xx} = \frac{\hat{\boldsymbol{P}}^2}{2M} + \frac{\hat{\boldsymbol{P}}_{12}^2}{2\mu_{12}} + \frac{\hat{\boldsymbol{p}}_1^2}{2\mu} + \frac{\hat{\boldsymbol{p}}_2^2}{2\mu} + V_{\text{Coul}} + \sum_{\boldsymbol{k}} \hbar\omega_0 a_{\boldsymbol{k}}^\dagger a_{\boldsymbol{k}} + \sum_{\boldsymbol{k}} [V_k a_{\boldsymbol{k}} \{\rho_{\boldsymbol{k}}(\boldsymbol{r}_1) e^{i\boldsymbol{k}\cdot\boldsymbol{R}_1} + \rho_{\boldsymbol{k}}(\boldsymbol{r}_2) e^{i\boldsymbol{k}\cdot\boldsymbol{R}_2}\} + \text{H.c.}], \tag{8}$$

where V_{Coul} is the Coulomb interaction between the particles, $\boldsymbol{R}_1 = \boldsymbol{R} + \frac{1}{2}\boldsymbol{R}_{12}$, $\boldsymbol{R}_2 = \boldsymbol{R} - \frac{1}{2}\boldsymbol{R}_{12}$, $M = 2M_x$ is the biexciton mass, and $\mu_{12} = \frac{M_x}{2}$ is the reduced mass of the exciton pair in the biexciton.

In the past [7,8] this problem was addressed using the wavefunction expressed as

$$|\Phi\rangle = e^{i(\boldsymbol{K}_1\cdot\boldsymbol{R}_1 + \boldsymbol{K}_2\cdot\boldsymbol{R}_2)} U_{xx} \phi(\boldsymbol{r}_1, \boldsymbol{r}_2, \boldsymbol{R}_{12})|0\rangle \tag{9}$$

with

$$U_{xx} = \exp\left[\sum_{\boldsymbol{k}} a_{\boldsymbol{k}} \{F_{\boldsymbol{k}}^{1*} e^{i\boldsymbol{k}\cdot\boldsymbol{R}_1} + F_{\boldsymbol{k}}^{2*} e^{i\boldsymbol{k}\cdot\boldsymbol{R}_2}\} - \text{H.c.}\right], \tag{10}$$

where U_{xx} is a generalization of the excitonic displacement operator U_x for a two-exciton system. The use of Eq. (8), however, posed a problem in eliminating the center-of-mass motion from the Hamiltonian. In addition, the biexcitonic orbital function, $\phi(\boldsymbol{r}_1, \boldsymbol{r}_2, \boldsymbol{R}_{12})$, was treated using simple functional forms that do not have enough variational degrees of freedom to accurately describe the Coulomb correlations of all particle pairs in the biexciton. In the present work, we propose a way to overcome these limitations.

We write the biexciton wave function using the translational motion operator T and the displacement operator U by analogy with the exciton:

$$|\Phi\rangle = TU\phi(\boldsymbol{r}_1, \boldsymbol{r}_2, \boldsymbol{R}_{12})|0\rangle. \tag{11}$$

The translational-motion operator is given by

$$T = \exp\left[i\left(\boldsymbol{Q} - \sum_{\boldsymbol{k}} \boldsymbol{k} a_{\boldsymbol{k}}^{\dagger} a_{\boldsymbol{k}}\right) \cdot \boldsymbol{R}\right], \tag{12}$$

where $\boldsymbol{Q} = \boldsymbol{P}/\hbar + \sum_{\boldsymbol{k}} \boldsymbol{k} a_{\boldsymbol{k}}^{\dagger} a_{\boldsymbol{k}}$, which is the total momentum of the biexciton-phonon system. As the total momentum of the system, $\boldsymbol{Q}$, is a constant of motion, the Hamiltonian transformed by the unitary operator depends on the total momentum $\boldsymbol{Q}$ only parametrically. In this work we are essentially interested in calculating the binding energy for a state at rest and hence we set $\boldsymbol{Q} = 0$. After transforming by the operator T, we have the Hamiltonian as

$$\begin{aligned} &T^{-1} H_{xx} T\big|_{\boldsymbol{Q}=0} \\ &= \frac{\hat{\boldsymbol{P}}_{12}^2}{2\mu_{12}} + \frac{\hat{\boldsymbol{p}}_1^2}{2\mu} + \frac{\hat{\boldsymbol{p}}_2^2}{2\mu} + V_{\text{Coul}} + \sum_{\boldsymbol{k}} \left\{\hbar\omega_0 + \frac{\hbar^2 k^2}{2M}\right\} a_{\boldsymbol{k}}^{\dagger} a_{\boldsymbol{k}} \\ &\quad + \sum_{\boldsymbol{k}} [V_k a_{\boldsymbol{k}} \{\rho_{\boldsymbol{k}}(\boldsymbol{r}_1) e^{\frac{i}{2}\boldsymbol{k}\cdot\boldsymbol{R}_{12}} + \rho_{\boldsymbol{k}}(\boldsymbol{r}_2) e^{-\frac{i}{2}\boldsymbol{k}\cdot\boldsymbol{R}_{12}}\} + \text{H.c.}]. \end{aligned} \tag{13}$$

We express the displacement operator as

$$U = U_x'\left(\boldsymbol{r}_1, \tfrac{1}{2}\boldsymbol{R}_{12}\right) U_x'\left(\boldsymbol{r}_2, -\tfrac{1}{2}\boldsymbol{R}_{12}\right), \tag{14}$$

with

$$\begin{aligned} &U_x'\left(\boldsymbol{r}, \frac{1}{2}\boldsymbol{R}_{12}\right) \\ &\quad = \exp\left[\sum_{\boldsymbol{k}} \left\{F_{\boldsymbol{k}}^*(\boldsymbol{r})\, a_{\boldsymbol{k}}\, e^{\frac{i}{2}\boldsymbol{k}\cdot\boldsymbol{R}_{12}} - F_{\boldsymbol{k}}(\boldsymbol{r})\, a_{\boldsymbol{k}}^{\dagger}\, e^{-\frac{i}{2}\boldsymbol{k}\cdot\boldsymbol{R}_{12}}\right\}\right], \end{aligned} \tag{15}$$

where $\frac{1}{2}\boldsymbol{R}_{12}$ $(-\frac{1}{2}\boldsymbol{R}_{12})$ corresponds to the center of mass of the exciton X_1 (X_2) in the biexciton in the rest frame of the $2e$-2h system. We apply the PB ansatz given by Eq. (7) to the phonon displacements $F_{\boldsymbol{k}}(\boldsymbol{r})$ in Eq. (15) and use the values corresponding to the $1s$ exciton as $f_{\boldsymbol{k}}^e$ and $f_{\boldsymbol{k}}^h$. This is justified by decomposition of the calculated biexciton wavefunction that shows the $1s$-exciton product state makes a dominating contribution, as discussed later.

Once operators T and U are written explicitly, an effective Hamiltonian for the biexciton with phonon coupling is readily obtained:

$$\mathcal{H} = \langle 0|U^{-1}T^{-1}H_{xx}TU|0\rangle = H_0 + V_{\text{eff}}, \tag{16}$$

where

$$V_{\text{eff}} = H_1 + H_2 \tag{17}$$

$$H_0 = -\frac{\hbar^2}{2\mu_{12}}\nabla_{\boldsymbol{R}_{12}}^2 - \frac{\hbar^2}{2\mu}\nabla_{\boldsymbol{r}_1}^2 - \frac{\hbar^2}{2\mu}\nabla_{\boldsymbol{r}_2}^2 + V_{\text{Coul}}, \tag{18}$$

$$\begin{aligned} H_1 = {} & 4\hbar\omega_0 \sum_{\boldsymbol{k}} |v_k|^2 \Big[-\left(f_{\boldsymbol{k}}^e + f_{\boldsymbol{k}}^h\right) \\ & + \frac{1}{2}\left(1 + R_e^2 k^2\right) f_{\boldsymbol{k}}^{e2} + \frac{1}{2}\left(1 + R_h^2 k^2\right) f_{\boldsymbol{k}}^{h2} \Big] \\ & + 2\hbar\omega_0 \sum_{\boldsymbol{k}} |v_k|^2 \left(f_{\boldsymbol{k}}^e + f_{\boldsymbol{k}}^h - f_{\boldsymbol{k}}^e f_{\boldsymbol{k}}^h\right) \\ & \times (\cos\boldsymbol{k}\cdot\boldsymbol{r}_1 + \cos\boldsymbol{k}\cdot\boldsymbol{r}_2), \end{aligned} \tag{19}$$

$$\begin{aligned} H_2 = {} & 2\hbar\omega_0 \sum_{\boldsymbol{k}} |v_k|^2 \\ & \times \Big[\left(-2f_{\boldsymbol{k}}^e + f_{\boldsymbol{k}}^{e2}\right) \cos\{\boldsymbol{k}\cdot(s_h\boldsymbol{r}_1 - s_h\boldsymbol{r}_2 + \boldsymbol{R}_{12})\} \\ & + \left(-2f_{\boldsymbol{k}}^h + f_{\boldsymbol{k}}^{h2}\right) \cos\{\boldsymbol{k}\cdot(s_e\boldsymbol{r}_1 - s_e\boldsymbol{r}_2 - \boldsymbol{R}_{12})\} \\ & + \left(f_{\boldsymbol{k}}^e + f_{\boldsymbol{k}}^h - f_{\boldsymbol{k}}^e f_{\boldsymbol{k}}^h\right) \cos\{\boldsymbol{k}\cdot(s_h\boldsymbol{r}_1 + s_e\boldsymbol{r}_2 + \boldsymbol{R}_{12})\} \\ & + \left(f_{\boldsymbol{k}}^e + f_{\boldsymbol{k}}^h - f_{\boldsymbol{k}}^e f_{\boldsymbol{k}}^h\right) \cos\{\boldsymbol{k}\cdot(s_e\boldsymbol{r}_1 + s_h\boldsymbol{r}_2 - \boldsymbol{R}_{12})\}\Big]. \end{aligned} \tag{20}$$

The fist term of Eq. (16), H_0, corresponds to the Hamiltonian describing the biexciton in the absence of coupling to phonons and the second term, V_{eff}, is an effective potential arising from the energy of the phonon cloud and the electron- and hole-phonon interactions.

It is instructive to compare the effective Hamiltonian of the biexciton with that of the exciton. The effective Hamiltonian for the $1s$ exciton coupled to phonons is given by

$$\mathcal{H}^x = \langle 0|U_x^{-1}T_x^{-1}H_xT_xU_x|0\rangle = H_0^x + V_{\text{eff}}^x, \tag{21}$$

where

$$V_{\text{eff}}^x = H_1^x, \tag{22}$$

$$H_0^x = -\frac{\hbar^2}{2\mu}\nabla_{\boldsymbol{r}}^2 - \frac{e^2}{\varepsilon_\infty r}, \tag{23}$$

$$\begin{aligned} H_1^x = {} & 2\hbar\omega_0 \sum_{\boldsymbol{k}} |v_k|^2 \Big[-\left(f_{\boldsymbol{k}}^e + f_{\boldsymbol{k}}^h\right) \\ & + \frac{1}{2}\left(1 + R_e^2 k^2\right) f_{\boldsymbol{k}}^{e2} + \frac{1}{2}\left(1 + R_h^2 k^2\right) f_{\boldsymbol{k}}^{h2} \Big] \\ & + 2\hbar\omega_0 \sum_{\boldsymbol{k}} |v_k|^2 \left(f_{\boldsymbol{k}}^e + f_{\boldsymbol{k}}^h - f_{\boldsymbol{k}}^e f_{\boldsymbol{k}}^h\right) \cos\boldsymbol{k}\cdot\boldsymbol{r}. \end{aligned} \tag{24}$$

Since $H_1(\boldsymbol{r}_1, \boldsymbol{r}_2) = H_1^x(\boldsymbol{r}_1) + H_1^x(\boldsymbol{r}_2)$, H_1 is due to the phonon coupling of each exciton in the biexciton. The additional term, H_2, in Eq. (17) can be interpreted as an interaction between the two excitons generated by phonon coupling.

B. Biexciton orbital wavefunction

Since the effective Hamiltonian $\mathcal{H}$ has been obtained as a form depending only on coordinates of electrons and holes, the biexciton orbital function $\phi(\boldsymbol{r}_1, \boldsymbol{r}_2, \boldsymbol{R}_{12})$ can be determined by the variational method. Expressing $\phi(\boldsymbol{r}_1, \boldsymbol{r}_2, \boldsymbol{R}_{12})$ in terms of basis functions φ_i,

$$\phi(\boldsymbol{r}_1, \boldsymbol{r}_2, \boldsymbol{R}_{12}) = \sum_i^K c_i \varphi_i(\boldsymbol{r}_1, \boldsymbol{r}_2, \boldsymbol{R}_{12}), \tag{25}$$

minimization of the expectation value of $\mathcal{H}$ with respect to variations of the parameters c_i leads to the following eigenvalue equation for the energy E, where K is the number of basis functions:

$$\sum_j^K \mathcal{H}_{ij} c_j = E \sum_j^K \mathcal{N}_{ij} c_j, \tag{26}$$

TABLE I. Ratios of biexciton binding energies to exciton binding energies with coupling to LO phonons neglected.

$\sigma = m_e/m_h$	0.1	0.5	1
Correlated Gaussian	0.156	0.0743	0.0640
Akimoto and Hanamura [21]	0.10[a]	0.034[a]	0.0273

[a]Values extracted from Fig. 1 of Ref. [21].

with

$$\mathcal{H}_{ij} = \int d\boldsymbol{r}\varphi_i^* \mathcal{H}\varphi_j \quad \text{and} \quad \mathcal{N}_{ij} = \int d\boldsymbol{r}\varphi_i^*\varphi_j, \tag{27}$$

where $d\boldsymbol{r} \equiv d\boldsymbol{r}_1 d\boldsymbol{r}_2 d\boldsymbol{R}_{12}$.

We write the basis function in terms of correlated Gaussians [11]:

$$\varphi_i(\boldsymbol{r}_1, \boldsymbol{r}_2, \boldsymbol{R}_{12}) = \mathcal{P} \exp\left\{-\frac{1}{2}\sum_{m,n=1}^{3} A_{mn}^{(i)} \boldsymbol{r}_m \cdot \boldsymbol{r}_n\right\}, \tag{28}$$

where $(\boldsymbol{r}_1, \boldsymbol{r}_2, \boldsymbol{r}_3) \equiv (\boldsymbol{r}_1, \boldsymbol{r}_2, \boldsymbol{R}_{12})$, $A^{(i)}$ is a 3×3 symmetric positive-definite matrix, and $\mathcal{P}$ is the symmetrizing operator with respect to exchange of the two excitons. Note that the correlated Gaussian includes cross terms, $A_{mn}^{(i)} \boldsymbol{r}_m \cdot \boldsymbol{r}_n$, which are essential to express correlations between the particles. Inclusion of several hundred Gaussian basis functions allows us to describe these correlations with high accuracy. Nonlinear variational parameters, $A_{nm}^{(i)}$, are determined by the stochastic variational method [9]; we prepare a huge number of K-dimensional basis sets $\{\varphi_1, \varphi_2, \ldots, \varphi_K\}$ as candidates, in which each basis function φ_i is expressed in terms of $A_{mn}^{(i)}$ generated randomly, calculate an eigenenergy with respect to each basis set by diagonalizing Eq. (25), and select the basis set yielding the lowest eigenenergy. The use of Gaussians as bases enables us to calculate the matrix elements $\mathcal{H}_{ij}$ and $\mathcal{N}_{ij}$ in a simple way and makes it relatively easy to use a large set of basis functions.

In earlier studies [21,22] the biexciton wavefunction was frequently represented by Hylleraas-type functions, which were employed for early studies of the positronium molecule, or its extensions. For example, Akimoto and Hanamura (AH) calculated the biexciton binding energy using an extended Hylleraas-type wavefunction for mass ratio $\sigma = m_e/m_h = 0$–1 excluding phonon coupling [21]. Such wavefunctions are grossly inadequate for capturing correlations of particle pairs in biexcitons. To test the correlated Gaussian basis functions, we calculated the biexciton binding energy using 200 basis functions neglecting phonons, that is, with $H = H_0$. Table I lists the ratios of the biexciton binding energies to those of exciton binding energies for $\sigma = 0.1$, 0.5, and 1. The calculation with correlated Gaussians yields considerably larger binding energies than that of AH for $\sigma = 0.1$–1. It is clear that the use of functional forms with a high degree of variational freedom such as in the correlated Gaussian basis is essential to obtain an accurate biexciton energy and wavefunction.

TABLE II. Material parameters and exciton energies for CuCl. Experimental values are deduced from exciton energies in Ref. [23] and the energy gap in Ref. [24]. Units of exciton energies are meV.

m_e	m_h	ε_0	ε_∞	$\hbar\omega_0$
$0.35m_0$	$1.95m_0$	6.1	3.7	25.6 meV
	$1s$	$2s$	$3s$	$4s$
$\langle H_x \rangle$	−318.5	−151.1	−131.1	−124.8
Binding energy	201.3	33.8	13.8	7.5 (calc)
	196.8	32.5	14.4	7.9 (expt)

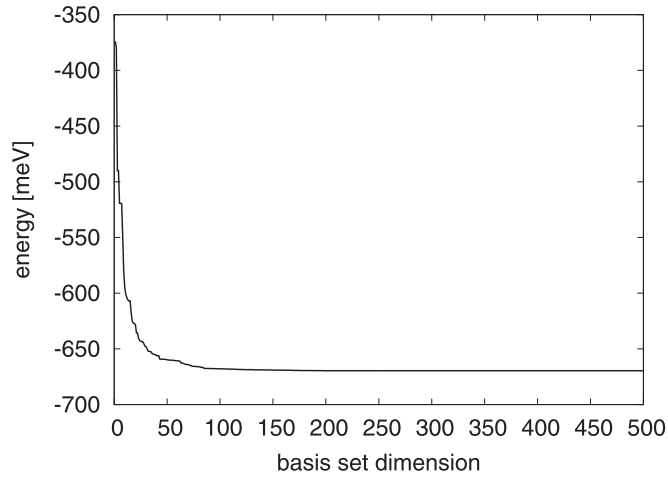

FIG. 2. Convergence of the eigenenergy of the biexciton with increasing basis set dimension.

Based on our previous work [10], we use $m_e + m_h = 2.3m_0$, $\sigma = 0.18$, $\varepsilon_0 = 6.1$, $\varepsilon_\infty = 3.7$, and $\omega_0 = 25.6$ meV as material parameters for CuCl, where m_0 is the free electron mass. These parameters were determined on the basis of available experimental data. The exciton binding energy is given by $-\langle H_x \rangle - \Sigma$, where Σ is the phonon self-energy of the free-electron–hole pair. $\Sigma = 117.3$ meV is obtained using the above parameters. Table II lists the used material parameters and the binding energies of the excitons in the ns states with $n = 1$–4. The calculated binding energies agree well with experimental binding energies.

III. BINDING ENERGY AND WAVE FUNCTION OF BIEXCITON

The biexciton total energy for CuCl is calculated to be $\langle \mathcal{H} \rangle = -669.6$ meV by the stochastic variational method with 500 correlated Gaussian basis functions [25]. Figure 2 shows the convergence of the eigenenergy of the biexciton with increasing basis set dimension. Table III lists the expectation values of various terms in the biexciton Hamiltonian $\mathcal{H}$. The phonon coupling in the two excitons in the biexciton, $\langle H_1 \rangle$,

TABLE III. Energy expectation values of the effective biexciton Hamiltonian in CuCl (in meV).

$\langle \mathcal{H} \rangle$	$\langle H_0 \rangle$	$\langle V_{\text{eff}} \rangle$	
−669.6	−625.2	−44.4	
		$\langle H_1 \rangle$	$\langle H_2 \rangle$
		−59.2	14.8

TABLE IV. Properties of the biexciton in CuCl. The length unit is in Å.

$\langle r_{eh}\rangle$	$\langle r_{ee}\rangle$	$\langle r_{hh}\rangle$	$\langle r_{XX}\rangle$
13.5	18.6	15.5	13.3
$\langle r_{eh}^2\rangle$	$\langle r_{ee}^2\rangle$	$\langle r_{hh}^2\rangle$	$\langle r_{XX}^2\rangle$
244	420	284	214
Δr_{eh}	Δr_{ee}	Δr_{hh}	Δr_{XX}
7.9	8.6	6.6	6.1
$\langle\delta(\boldsymbol{r}_{eh})\rangle$	$\langle\delta(\boldsymbol{r}_{ee})\rangle$	$\langle\delta(\boldsymbol{r}_{hh})\rangle$	$\langle\delta(\boldsymbol{r}_{XX})\rangle$
5.89×10^{-4}	2.80×10^{-5}	4.63×10^{-6}	3.56×10^{-5}

is attractive, while the interaction between the two excitons generated by phonon coupling, $\langle H_2\rangle$, is repulsive. The total effective potential $\langle V_{\rm eff}\rangle$ is negative and accounts for 6.6% of the total energy. The resulting biexciton binding energy, $2\langle H_x\rangle_{1s} - \langle\mathcal{H}\rangle$, is 32.6 meV, where $\langle H_x\rangle_{1s}$ (= −318.5 meV) is the 1*s* exciton energy. Here we have not included the electron-hole exchange interaction. In the next section we discuss the correction to the binding energy due to the electron-hole (*e*-h) exchange interaction.

Properties of the biexciton in CuCl are obtained from the wavefunction calculated by the above variational procedure. Table IV lists properties relating to particle distribution, where $\Delta r_{ij} \equiv \sqrt{\langle r_{ij}^2\rangle - \langle r_{ij}\rangle^2}$ is the standard deviation of the distance between particles i and j and $\langle\delta(\boldsymbol{r}_{ij})\rangle$ is the probability that i and j are located at a same position. The standard deviation $\Delta r_{hh} = 6.6$ Å is less than 80% of Δr_{ee}. This small fluctuation of the hole-hole (h-h) distance is reasonable from the fact that the hole is considerably heavier than the electron for CuCl. $\Delta r_{XX} = 6.1$ Å is comparable to Δr_{hh}, where the two-exciton distance, r_{XX}, corresponds to the distance between the centers of masses of two excitons, that is, $r_{XX} = R_{12}$. The comparable fluctuation of X-X distance is because the center of mass of the exciton is close to the hole due to a large mass of the hole.

Further details of the biexciton wavefunction can be obtained by calculating two-particle correlation functions defined by

$$\mathcal{C}_{ij}(\boldsymbol{r}) = \int d\boldsymbol{r}_1 d\boldsymbol{r}_2 d\boldsymbol{R}_{12}\delta(\boldsymbol{r}-\boldsymbol{r}_{ij})|\Phi(\boldsymbol{r}_1,\boldsymbol{r}_2,\boldsymbol{R}_{12})|^2, \quad (29)$$

where $\boldsymbol{r}_{ij}$ is the relative coordinate between particles i and j. $\mathcal{C}_{ij}(\boldsymbol{r})$ corresponds to the probability density that the particle

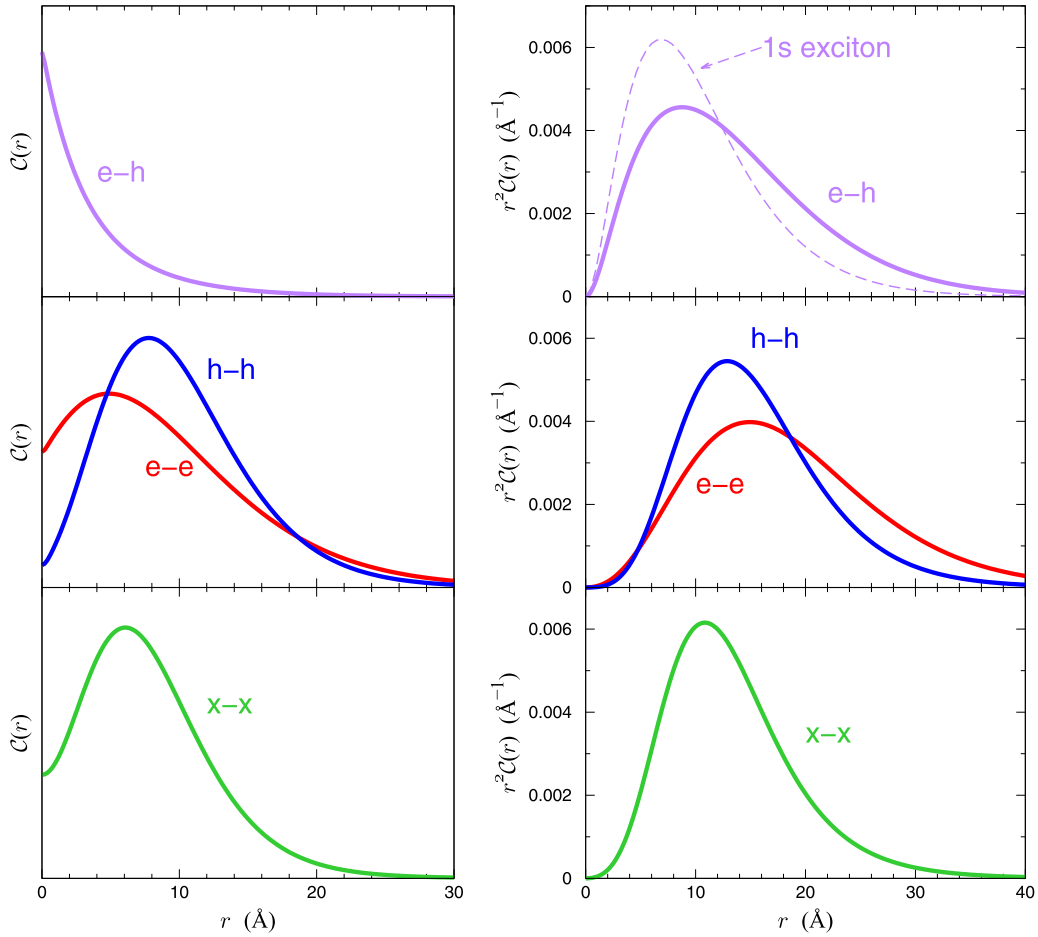

FIG. 3. Two-particle correlations for *e*-h, h-h, *e*-*e*, and X-X. The left figures show $\mathcal{C}_{ij}(\boldsymbol{r})$ in an arbitrary unit. The peak positions of $\mathcal{C}_{ij}(\boldsymbol{r})$ for h-h, *e*-*e*, and X-X are 7.8, 4.9, and 6.1 Å, respectively. The right figures show $r^2\mathcal{C}_{ij}(\boldsymbol{r})$. The peak positions of $r^2\mathcal{C}_{ij}(\boldsymbol{r})$ for *e*-h, h-h, *e*-*e*, and X-X are 8.8, 12.9, 14.9, and 10.8 Å, respectively.

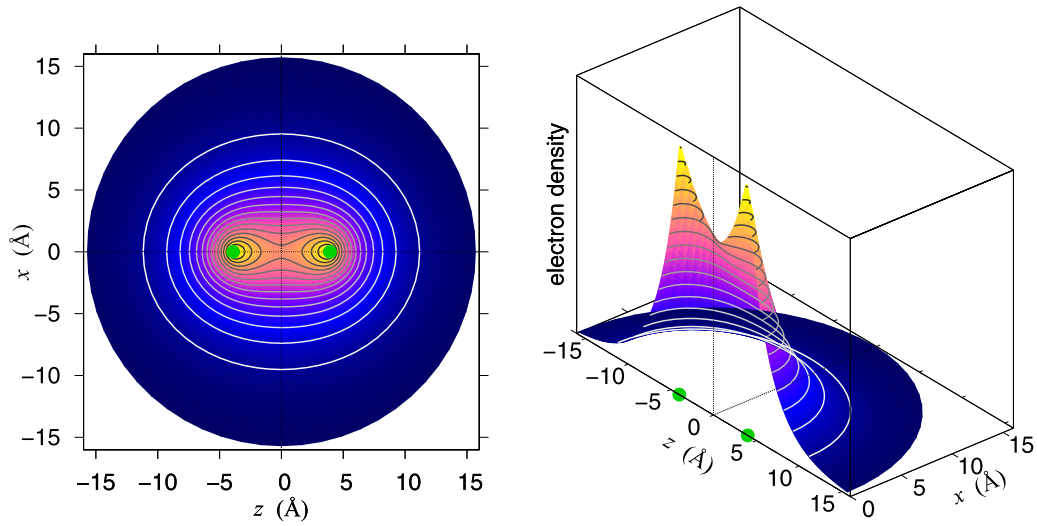

FIG. 4. The electron density distribution for a fixed h-h distance $r_{hh}^0 = 7.8$ Å. The left and right figures are a two-dimensional contour map and a three-dimensional plot of the electron density, respectively. The cusp positions are represented by green dots.

i is located at $\boldsymbol{r}$ from the particle j. Since the ground-state biexciton wavefunction has spherical symmetry, $\mathcal{C}_{ij}(\boldsymbol{r})$ is also spherical. Figure 3 shows the correlations with respect to the e-h, electron-electron (e-e), h-h, and two-exciton distances. The panels on the left in Fig. 3 show $C_{ij}(\boldsymbol{r})$, whose value at $\boldsymbol{r} = 0$ corresponds to $\langle\delta(\boldsymbol{r}_{ij})\rangle$ in Table IV. The right panels show $r^2 C_{ij}(\boldsymbol{r})$, which is equivalent to the radial probability density. The e-h correlation is shown in the top panels in Fig. 3. $\mathcal{C}_{eh}(\boldsymbol{r})$ has a cusp at $r = 0$ as is common with the hydrogen atom and an exciton. The radial probability density $r^2\mathcal{C}_{eh}(r)$ reaches a maximum at $r = 8.8$ Å and is more widely distributed than that of the $1s$ exciton, $r^2\psi_{1s}^2$, which has a maximum at $a_X = 6.9$ Å. The h-h and e-e correlations are shown in the middle panels in Fig. 3. $\mathcal{C}_{hh}(\boldsymbol{r})$ is relatively localized at $r_{hh} = 7.8$ Å and is considerably suppressed at $r_{hh} = 0$ compared to $\mathcal{C}_{ee}(\boldsymbol{r})$. The distribution of the h-h correlation function provides understanding that the two holes in the biexciton are narrowly distributed away from each other at a distance of about 7.8 Å. The two-exciton correlation is shown in the bottom panels in Fig. 3.

The electron density for a fixed h-h distance r_{hh}^0 is defined by

$$\mathcal{C}_e^{r_{hh}^0}(\boldsymbol{r}) = \int d\boldsymbol{r}_1 d\boldsymbol{r}_2 d\boldsymbol{R}_{12}\, \delta(\boldsymbol{r} - \boldsymbol{r}_e)\, \delta\left(\boldsymbol{r}_{hh} - \boldsymbol{r}_{hh}^0\right) \times |\Phi(\boldsymbol{r}_1, \boldsymbol{r}_2, \boldsymbol{R}_{12})|^2. \tag{30}$$

We calculated the electron density $\mathcal{C}_e^{r_{hh}^0}(\boldsymbol{r})$ with $\boldsymbol{r}_{hh}^0 = 7.8\,\text{Å}\hat{z}$, which is cylindrically symmetric about the z axis. Figure 4 shows $\mathcal{C}_e^{r_{hh}^0}(r)$ on the xz plane in two ways: the left figure is a contour map and the right is an electron density plot. The electron density has two cusps on the z axis (green dots) and the distance between them corresponds to the h-h distance $r_{hh}^0 = 7.8$ Å. This supports the presumption that the biexciton is predominantly formed of two $1s$ excitons.

IV. ELECTRON-HOLE EXCHANGE IN EXCITON AND BIEXCITON

In this section we discuss the contribution of the electron-hole exchange interaction to the binding energies of the biexciton in CuCl. To do so, we must estimate the e-h exchange energies of the exciton as well as the biexciton.

The e-h exchange interaction can be separated into a short-range term and a long-range term. For the exciton, the short-range exchange raises the energy of the spin-singlet state, whereas the long-range exchange is responsible for the longitudinal-transverse (LT) splitting of the singlet state, as shown in Fig. 5. Thus, the short-range exchange energy is expressed as

$$E_{\text{s.r.}}^X = E_T - E_{\text{tri}} + \tfrac{1}{3}\Delta E_{LT}, \tag{31}$$

where $\Delta E_{LT} \equiv E_L - E_T$ is the LT splitting energy, E_T and E_L are the transverse and longitudinal exciton energies, respectively, and E_{tri} is the triplet exciton energy.

We note that the observed longitudinal exciton energy is shifted from E_L in practice. This shift results from polariton coupling combining a longitudinal exciton with longitudinal excitons from higher bands. The $1s$ Z_3 longitudinal exciton couples dominantly to the $1s$ Z_{12} longitudinal exciton and, in

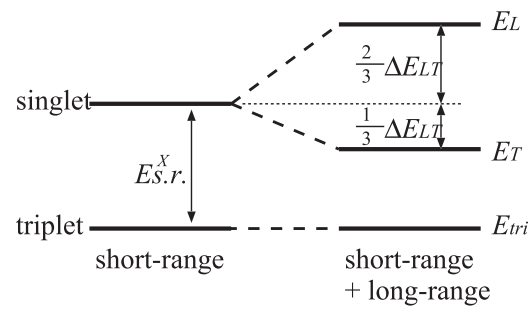

FIG. 5. Schematic of e-h exchange of an exciton. E_T and E_L are the transverse and longitudinal exciton energies, respectively, and E_{tri} is the spin-triplet exciton energy.

TABLE V. Measured exciton excitation energies for CuCl (in eV).

$Z_3(1s)$	triplet	$E_{\rm tri}$	3.1997 [27]
	transverse	E_T	3.2022 [26,28]
	longitudinal	E'_L	3.2079 [26,28]
$Z_{12}(1s)$	transverse	E_t	3.267 [26]
	longitudinal	E'_l	3.2896 [26]

consequence the $1s$ Z_3 and Z_{12} longitudinal exciton energies shift downward and upward, respectively, from their uncoupled (calculated) values. Thus, the observed LT separation is smaller than that resulting from the long-range exchange, ΔE_{LT}. The calculated Z_3 longitudinal exciton energy, E_L, relates to the observed Z_3 and Z_{12} longitudinal exciton energies, denoted by E'_L and E'_l, respectively, as [26]

$$E_L = \sqrt{E'^2_L + \frac{\left(E'^2_l - E_t^2\right)\left(E'^2_L - E_T^2\right)}{E_t^2 - E_T^2}}. \tag{32}$$

Here E_T and E_t correspond to the Z_3 and Z_{12} transverse exciton energies, respectively. Using Eqs. (31) and (32), and the measured excitation energies in Table V, we obtain $\Delta E_{LT} = 7.7$ meV and $E^X_{\rm s.r.} = 5.1$ meV, which are listed in Table VI.

For the biexciton, the short-range exchange contribution to the Hamiltonian is given by [29]

$$H^{XX}_{\rm s.r.} = \frac{3}{4}\frac{E^X_{\rm s.r.}}{|\psi_{1s}(0)|^2}\{\delta(\mathbf{r}_{e1}-\mathbf{r}_{h1}) + \delta(\mathbf{r}_{e1}-\mathbf{r}_{h2}) + \delta(\mathbf{r}_{e2}-\mathbf{r}_{h1}) + \delta(\mathbf{r}_{e2}-\mathbf{r}_{h2})\}, \tag{33}$$

where $\psi_{1s}(r)$ is the orbital function of the $1s$ exciton. By calculating the expectation value of $H^{XX}_{\rm s.r.}$ in the biexciton ground state, we obtain the exchange energy of the biexciton as $E^{XX}_{\rm s.r.} = 1.74E^X_{\rm s.r.}$.

On the other hand, the long-range exchange term for the biexciton can be argued to be absent as follows. The long-range exchange term describes the long-range Coulomb dipole-dipole coupling between excitonic excitations at different sites in the crystal. In case of the biexciton, as the e-h pairs can create and annihilate only within a size of the biexciton, there is no contribution from long-range Coulomb coupling. More rigorously, the long-range dipole-dipole interaction energy for a spherically symmetric biexciton state can be calculated exactly and shown to vanish. A proof is given in the Appendix.

As a result, including the electron-hole exchange, excitation energies of the Z_3 transverse exciton and the biexciton

TABLE VI. Energy corrections due to exchange interaction for CuCl (in meV).

Exciton	$E^X_{\rm s.r.}$	5.1 meV
	ΔE_{LT}	7.7 meV
Biexciton	$E^{XX}_{\rm s.r.}$	8.9 meV
	long-range	~ 0
Biexciton binding energy correction	Δ_{XX}	-3.8 meV

TABLE VII. Comparison of the biexciton binding energy ΔE_{BX} calculated by various authors and the present work. The values referred to as previous works are extracted from figures in original papers for $\sigma = 0.18$.

	ΔE_{BX} (meV)
Previous work	
extended Hylleraas-type[a]	14
extended Hylleraas-type[b]	15
correlated Gaussian[c]	24
Present work	
with phonon effect	32.6
with phonon + e-h exchange	28.8
Experiment	32

[a]Akimoto and Hanamura [21].
[b]Brinkman, Rice and Bell [22].
[c]Usukura, Suzuki, and Varga [9].

are given by

$$E_x = \langle \mathcal{H}_x\rangle_{1s} + E^X_{\rm s.r.} + \tfrac{1}{3}\Delta E_{LT} + E_g \tag{34}$$

and

$$E_{xx} = \langle \mathcal{H}\rangle + 1.74E^X_{\rm s.r.} + 2E_g, \tag{35}$$

respectively, where E_g is the gap energy. Therefore, the biexciton binding energy, $E^{XX}_b = 2E_x - E_{xx}$, is obtained from

$$E^{XX}_b = (2\langle H_x\rangle_{1s} - \langle \mathcal{H}\rangle) + \Delta_{XX}, \tag{36}$$

with

$$\Delta_{XX} = 0.26E^X_{\rm s.r.} - \tfrac{2}{3}\Delta E_{LT}. \tag{37}$$

The first term of Eq. (36) corresponds to the biexciton binding energy excluding the e-h exchange interaction calculated variationally as 32.6 meV in the previous section. The second term Δ_{XX} is the contribution of the electron-hole exchange interactions to the binding energy of the biexciton and is estimated to be -3.8 meV. Therefore, the biexciton binding energy including the exchange energy is obtained as 28.8 meV. This compares well with the experimental binding energy [13] of 32 meV. We stress that the correction due to e-h exchange is more than 10% of the biexciton binding energy and is not a negligible contribution.

V. CONCLUSIONS

A method for describing the biexciton with both Coulomb coupling between the electron-hole pairs and their coupling to phonons was developed and applied to calculate the energy and correlation functions of the biexciton in CuCl. We derived an effective Hamiltonian for the biexciton using a form of the orbital wave function that is translationally invariant and a coherent state for the phonon cloud dressing the electron-hole pairs. This allowed the use of sophisticated variational functions for constructing the orbital wave function of the biexciton.

Table VII compares the biexciton binding energy calculated in the present work with that calculated without the phonon effect in previous works. Since the ratio of the biexciton binding energy to that of the exciton as a function of σ

was reported in original articles of previous works, we used the values for $\sigma = 0.18$ and multiplied them by the experimental exciton binding energy $\Delta E_x = 197$ meV for the data in the table. Calculation using correlated Gaussians yields ΔE_{BX} 60% larger than those using the extended Hylleraas-type wavefunctions. However, even with the use of correlated Gaussians ΔE_{BX} is underestimated by 25% compared to the experimental value when we neglect the phonon effect. This is largely due to the wrong interpretation of exciton binding energy as the exciton Rydberg (measure of the Coulomb interaction in the exciton) as discussed by us previously in Ref. [10]. Furthermore, for an accurate description of the biexciton, it is necessary to include the coupling to phonons.

The present work using correlated Gaussians and with the inclusion of phonon coupling leads to ΔE_{BX} of 32.6 meV in CuCl. The contribution of the electron-hole exchange interaction to the exciton and biexciton energies were also estimated. ΔE_{BX} is reduced by 3.8 meV due to exchange interaction. As a result, ΔE_{BX} in CuCl is 28.8 meV, which compares well with the experimental value of 32 meV.

To account for the remaining difference between theory and experiment, we point to approximations inherent in the present work. We have simplified the phonon part of the biexciton wave function using the displacement amplitude of two $1s$ excitons. If the displacement amplitude for the biexciton is treated as a variational function, ΔE_{BX} would somewhat increase. Moreover, use of a continuum effective-mass-based model implies that we do not include any so-called central cell corrections due to the atomistic nature of the crystal structure that would modify the Coulomb interaction when the interacting particles are in the same unit cell. Since the sizes of the $1s$ exciton and biexciton are comparable to that of the unit cell in CuCl, the central cell corrections may not be negligible. However, ΔE_{BX} is estimated from the difference between the total energy of the biexciton and twice the exciton total energy and both of these could be considered to have similar central cell corrections. Therefore, the central cell correction in ΔE_{BX} may be not as important as for the 1s exciton due to its cancellation in the first-order approximation.

The behavior of the wavefunction of the biexciton can be explored using the correlation functions between particles. We showed that holes are relatively localized in the biexciton although the correlation between the holes cannot be neglected. It is also found that the electron distribution spreads widely surrounding the two holes.

The details of biexciton wave function can also contribute to the understanding of its creation and decay processes. The biexciton creation by two-photon absorption is often explained using the giant oscillator strength (GOS) model [30], which predicts an enhanced transition rate from exciton to biexciton because of the large spatial extension of the latter. Using a simple form for the wavefunction expressed in terms of the product of two exciton wavefunctions, the transition rate derived from the GOS model is proportional to $(a_B/a_X)^3$, where a_B is the average distance between the two excitons in the biexciton state. A large enhancement of the transition rate was concluded from $a_B \sim 3a_X$ estimated using the average h-h distance calculated in Ref. [21]. On the other hand, our calculation yields the average two-exciton distance $\langle r_{XX} \rangle$ as $1.9a_X = 13.3$ Å and the peak X-X distances of $\mathcal{C}_{XX}$ and $r^2\mathcal{C}_{XX}$ as $0.9a_X = 6.1$ Å and $1.6a_X = 10.8$ Å, respectively. These would indicate that the enhancement of the transition rate due to the GOS model may be much smaller than anticipated in the earlier study. In addition, the interparticle correlations captured in our superposition of correlated Gaussians is much more complex than assumed in previous models and the transition rate cannot be expressed in terms of a single parameter describing the extension of the biexciton. Furthermore, the validity of the GOS model itself has been questioned as the biexciton state lies in the continuum of two excitonic polaritons and a bipolariton model has been proposed [31,32]. The availability of an accurate biexciton wavefunction presented here can enable a thorough quantitative analysis of the biexciton creation and decay processes. This will be addressed in a future publication.

ACKNOWLEDGMENTS

This collaboration work started at JST, ERATO MASUMOTO Single Quantum Dot Project. We would like to thank Prof. Yasuaki Masumoto for his support and many useful discussions during the project.

APPENDIX: LONG-RANGE EXCHANGE OF THE BIEXCITON

The biexciton state is constructed out of products of a two-electron state of spin zero and a two-hole state of total angular momentum zero (singlet-singlet product):

$$\tfrac{1}{2}\Phi_{\boldsymbol{r}_{e_1}\boldsymbol{r}_{h_1}\boldsymbol{r}_{e_2}\boldsymbol{r}_{h_2}}\left\{\left|\uparrow \tfrac{1}{2}\right\rangle\left|\downarrow -\tfrac{1}{2}\right\rangle - \left|\uparrow -\tfrac{1}{2}\right\rangle\left|\downarrow \tfrac{1}{2}\right\rangle - \left|\downarrow \tfrac{1}{2}\right\rangle\left|\uparrow -\tfrac{1}{2}\right\rangle + \left|\downarrow -\tfrac{1}{2}\right\rangle\left|\uparrow \tfrac{1}{2}\right\rangle\right\}. \tag{A1}$$

Here we explicitly derive the expectation value of long-range exchange interaction only between e_2 and h_2 as those for other e-h pair combinations can be obtained similarly. The expectation value of the long-range exchange between e_2 and h_2 with respect to the singlet-singlet biexciton is given by

$$\langle V_{LR}\rangle = \tfrac{1}{4}\left[\left\langle V_{LR}{}^{\uparrow 1/2}_{\uparrow 1/2}\right\rangle + \left\langle V_{LR}{}^{\uparrow -1/2}_{\uparrow -1/2}\right\rangle + \left\langle V_{LR}{}^{\downarrow 1/2}_{\downarrow 1/2}\right\rangle + \left\langle V_{LR}{}^{\downarrow -1/2}_{\downarrow -1/2}\right\rangle\right], \tag{A2}$$

with

$$\left\langle V_{LR}{}^{\mu\nu}_{\mu'\nu'}\right\rangle = \sum_{\boldsymbol{r}_{e_1}\boldsymbol{r}_{h_1}\boldsymbol{r}_{e_2}\boldsymbol{r}'_{e_2}}{}' \Phi^*_{\boldsymbol{r}_{e_1}\boldsymbol{r}_{h_1}\boldsymbol{r}_{e_2}\boldsymbol{r}_{e_2}} \boldsymbol{d}^{\mu\nu} \frac{I - 3\boldsymbol{n}\boldsymbol{n}}{\left|\boldsymbol{r}_{e_2} - \boldsymbol{r}'_{e_2}\right|^3} \boldsymbol{d}^{\nu'\mu'} \Phi_{\boldsymbol{r}_{e_1}\boldsymbol{r}_{h_1}\boldsymbol{r}'_{e_2}\boldsymbol{r}'_{e_2}}, \tag{A3}$$

where $\mu(\nu)$ denotes the spin (total angular momentum) index of the conduction (valence) band occupied by e_2 (h_2) and $\sum'$ stands for the summation over $\boldsymbol{r}_{e_2}$ and $\boldsymbol{r}'_{e_2}$ excluding the point $\boldsymbol{r}_{e_2} = \boldsymbol{r}'_{e_2}$. In Eq. (A3) I is the unit dyadic, $\boldsymbol{n}$ is a unit vector defined by $\boldsymbol{n} = (\boldsymbol{r}_{e_2} - \boldsymbol{r}'_{e_2})/|\boldsymbol{r}_{e_2} - \boldsymbol{r}'_{e_2}|$, and $\boldsymbol{d}$ is the interband dipole moment

$$\boldsymbol{d}^{\mu\nu} = e\int d^3r\; w^*_{c\mu}(\boldsymbol{r})\boldsymbol{r}w_{v\nu}(\boldsymbol{r}), \tag{A4}$$

where $w_{c\mu}$ ($w_{v\nu}$) denotes the Wannier orbital for conduction (valence) band μ (ν). Equation (A3) is the dipole term in the multipole expansion of the long-range exchange, where the monopole term vanishes and higher-order terms are neglected.

Converting Eq. (A3) into continuum representation,

$$\begin{aligned}\left\langle V_{LR}{}^{\mu\nu}_{\mu'\nu'}\right\rangle &= -\frac{4\pi}{3}\boldsymbol{d}^{\mu\nu}\cdot\boldsymbol{d}^{\nu\mu}\int d^3r_{e_1}\, d^3r_{h_1}\, d^3r\left|\phi^*\left(\boldsymbol{r}_{e_1},\boldsymbol{r}_{h_1},\boldsymbol{r},\boldsymbol{r}\right)\right|^2 \\ &+\int d^3r_{e_1}d^3r_{h_1}d^3r\boldsymbol{d}^{\mu\nu}\cdot\left(\nabla_r\phi^*\left(\boldsymbol{r}_{e_1},\boldsymbol{r}_{h_1},\boldsymbol{r},\boldsymbol{r}\right)\right) \\ &\times\boldsymbol{d}^{\nu'\mu'}\cdot\nabla_r\int d^3r'\,\frac{1}{|\boldsymbol{r}-\boldsymbol{r}'|}\phi\left(\boldsymbol{r}_{e_1},\boldsymbol{r}_{h_1},\boldsymbol{r}',\boldsymbol{r}'\right),\end{aligned}\tag{A5}$$

where $\phi(\boldsymbol{r}_{e_1},\boldsymbol{r}_{h_1},\boldsymbol{r}'_{e_2},\boldsymbol{r}'_{h_2}) = \Phi_{\boldsymbol{r}_{e_1}\boldsymbol{r}_{h_1}\boldsymbol{r}'_{e_2}\boldsymbol{r}'_{h_2}}/\Omega^2$ and Ω is the volume of the unit cell. Here we have used the relation [33]

$$\begin{aligned}\int_\sigma d^3r'\ \text{grad div}\,\frac{\boldsymbol{Q}(\boldsymbol{r}')}{|\boldsymbol{r}-\boldsymbol{r}'|} &= \text{grad div}\int_\sigma d^3r'\frac{\boldsymbol{Q}(\boldsymbol{r}')}{|\boldsymbol{r}-\boldsymbol{r}'|}-\frac{4\pi}{3}\boldsymbol{Q}(\boldsymbol{r}),\end{aligned}\tag{A6}$$

where $\boldsymbol{Q}$ is any vector field and σ denotes the surface of a small excluded volume around $\boldsymbol{r}=\boldsymbol{r}'$.

Transforming to relative and center-of-mass coordinates, the wavefunction of the biexciton may be expressed as

$$\phi_(\boldsymbol{r}_{e1},\boldsymbol{r}_{h1},\boldsymbol{r}_{e2},\boldsymbol{r}_{h2}) = \frac{1}{\sqrt{\Omega}}\varphi(\boldsymbol{r}_1,\boldsymbol{r}_2,\boldsymbol{R}_{12})e^{i\boldsymbol{K}\cdot\boldsymbol{R}},\tag{A7}$$

where the coordinates, $\boldsymbol{r}_1$, $\boldsymbol{r}_2$, $\boldsymbol{R}_{12}(=\boldsymbol{R}_1-\boldsymbol{R}_2)$ and $\boldsymbol{R}$, are defined as in Fig. 1. The integral over coordinates $(\boldsymbol{r}_{e_1},\boldsymbol{r}_{h_1},\boldsymbol{r},\boldsymbol{r}')$ in Eq. (A5) may be rewritten as an integral over $(\boldsymbol{r}_1,\boldsymbol{R}_{12},\boldsymbol{R}'_{12},\boldsymbol{R})$. The coordinates $\boldsymbol{r}$ and $\boldsymbol{r}'$ in Eq. (A5) correspond to $\boldsymbol{R}_2$ and $\boldsymbol{R}'_2$, respectively. Since $\boldsymbol{R}_{12}$ and $\boldsymbol{R}$ are expressed in terms of $\boldsymbol{R}_1$ and $\boldsymbol{R}_2$ as

$$\boldsymbol{R}_{12}=\boldsymbol{R}_1-\boldsymbol{R}_2\quad\text{and}\quad\boldsymbol{R}=\tfrac{1}{2}\boldsymbol{R}_1+\tfrac{1}{2}\boldsymbol{R}_2,\tag{A8}$$

and $\nabla_r = -\nabla_{R_{12}}+\frac{1}{2}\nabla_R$, Eq. (A5) becomes

$$\begin{aligned}\left\langle V_{LR}{}^{\mu\nu}_{\mu'\nu'}\right\rangle &= -\frac{4\pi}{3}\boldsymbol{d}^{\mu\nu}\cdot\boldsymbol{d}^{\nu'\mu'}\int d^3r_1\, d^3R_{12}\,|\varphi(\boldsymbol{r}_1,0,\boldsymbol{R}_{12})|^2 \\ &+\int d^3r_1\, d^3R_{12}\,\boldsymbol{d}^{\mu\nu}\cdot(\nabla_R\varphi^*(\boldsymbol{r}_1,0,\boldsymbol{R}_{12})) \\ &\times\boldsymbol{d}^{\nu'\mu'}\cdot\nabla_{R_{12}}\int d^3R'_{12}\,\frac{1}{|\boldsymbol{R}_{12}-\boldsymbol{R}'_{12}|}\varphi(\boldsymbol{r}_1,0,\boldsymbol{R}'_{12}),\end{aligned}\tag{A9}$$

where we used $\boldsymbol{R}_2-\boldsymbol{R}'_2=\boldsymbol{R}_{12}-\boldsymbol{R}'_{12}$.

We introduce a Fourier representation of $\varphi(\boldsymbol{r}_1,0,\boldsymbol{R}_{12})$ for its R_{12} dependence,

$$\varphi(\boldsymbol{r}_1,0,\boldsymbol{R}_{12}) = \frac{1}{\sqrt{8\pi^3}}\int d^3k\varphi_{\boldsymbol{k}}(\boldsymbol{r}_1,0)\exp(i\boldsymbol{k}\cdot\boldsymbol{R}_{12}).\tag{A10}$$

with $\varphi_{\boldsymbol{k}}(\boldsymbol{r}_1,0)$ normalized as $\int d^3k|\varphi_{\boldsymbol{k}}(\boldsymbol{r}_1,0)|^2=1$. Substituting Eq. (A10) in Eq. (A9), we obtain

$$\begin{aligned}\left\langle V_{LR}{}^{\mu\nu}_{\mu'\nu'}\right\rangle &= -\frac{4\pi}{3}\sum_i d_i^{\mu\nu}d_i^{\nu'\mu'}\int d^3r_1\, d^3R_{12}\, d^3k\,|\varphi_{\boldsymbol{k}}(\boldsymbol{r}_1,0)|^2 \\ &+4\pi\int d^3r_1\, d^3R_{12}\sum_{ij}d_i^{\mu\nu}d_j^{\nu'\mu'} \\ &\times\int d^3k\,\frac{k_ik_j}{k^2}\,|\varphi_{\boldsymbol{k}}(\boldsymbol{r}_1,0)|^2.\end{aligned}\tag{A11}$$

Since $\varphi(\boldsymbol{r}_1,0,\boldsymbol{R}_{12})$ is a spherically symmetric state, $|\varphi_{\boldsymbol{k}}(\boldsymbol{r}_1,0)|^2$ is also spherically symmetric with respect to $\boldsymbol{k}$. Replacing the momentum index of $\varphi_{\boldsymbol{k}}(\boldsymbol{r}_1,0)$ with scalar k,

$$\begin{aligned}\left\langle V_{LR}{}^{\mu\nu}_{\mu'\nu'}\right\rangle &= -\frac{4\pi}{3}\sum_i d_i^{\mu\nu}d_i^{\nu'\mu'}\int d^3r_1\, d^3R_{12}\, d^3k\,|\varphi_k(\boldsymbol{r}_1,0)|^2 \\ &+4\pi\int d^3r_1\, d^3R_{12}\int d^3k\sum_{ij}d_i^{\mu\nu}d_j^{\nu'\mu'}\frac{k_ik_j}{k^2}\,|\varphi_k(\boldsymbol{r}_1,0)|^2.\end{aligned}\tag{A12}$$

In the angular averages of k_ik_j/k^2 terms with $i\neq j$ vanish and the k_i^2/k^2 terms average to $1/3$ since $\int d^3k\frac{k_x^2}{k^2}|\phi_k|^2 = \int d^3k\frac{k_y^2}{k^2}|\phi_k|^2 = \int d^3k\frac{k_z^2}{k^2}|\phi_k|^2$ so that

$$\begin{aligned}\left\langle V_{LR}{}^{\mu\nu}_{\mu'\nu'}\right\rangle &= -\frac{4\pi}{3}\sum_i d_i^{\mu\nu}d_i^{\nu'\mu'}\int d^3r_1\, d^3R_{12}\, d^3k\,|\varphi_k(\boldsymbol{r}_1,0)|^2 \\ &+\frac{4\pi}{3}\int d^3r_1\, d^3R_{12}\sum_i d_i^{\mu\nu}d_i^{\nu'\mu'}\int d^3k \\ &\times\frac{k_x^2+k_y^2+k_z^2}{k^2}\,|\varphi_k(\boldsymbol{r}_1,0)|^2.\end{aligned}\tag{A13}$$

The second term cancels the first term and $\langle V_{LR}{}^{\mu\nu}_{\mu'\nu'}\rangle = 0$. Therefore, the long-range exchange energy of the biexciton vanishes. Note that this is valid for any spin-zero state that is rotationally invariant (isotropic).

[1] H. Haken, Z. Phys. **146**, 527 (1956).
[2] M. Matsuura and H. Büttner, Phys. Rev. B **21**, 679 (1980).
[3] M. Matsuura and H. Büttner, Solid State Commun. **33**, 221 (1980).
[4] J. Pollmann and H. Büttner, Solid State Commun. **17**, 1171 (1975).
[5] E. O. Kane, Phys. Rev. B **18**, 6849 (1978).
[6] J. Pollmann and H. Büttner, Phys. Rev. B **16**, 4480 (1977).
[7] P. P. Schmidt, J. Phys. C **2**, 785 (1969).
[8] J. Pollmann and H. Büttner, Solid State Commun. **12**, 1105 (1973).
[9] J. Usukura, Y. Suzuki, and K. Varga, Phys. Rev. B **59**, 5652 (1999).
[10] S. V. Nair, J. Usukura, and E. Tokunaga, Phys. Rev. B **102**, 075202 (2020).
[11] K. Varga, J. Usukura, and Y. Suzuki, Phys. Rev. Lett. **80**, 1876 (1998).
[12] M. Ueta, H. Kanzaki, K. Kobayashi, Y. Toyozawa, and E. Hanamura, *Excitonic Processes in Solids*, Springer Series in

Solid-State Sciences Vol. 60 (Springer-Verlag, Berlin, 1986), Chaps. 2 and 3.
[13] G. Gale and A. Mysyrowicz, Phys. Rev. Lett. **32**, 727 (1974).
[14] B. Hönerlage, C. Klingshirn, and J. B. Grun, Phys. Status Solidi B **78**, 599 (1976).
[15] T. Itoh, Y. Iwabuchi, and M. Kataoka, Phys. Status Solidi B **145**, 567 (1988).
[16] I. Henneberger, K. Henneberger, and J. Voigt, Phys. Status Solidi B **83**, 439 (1977).
[17] H. Akiyama, T. Kuga, M. Matsuoka, and M. Kuwata-Gonokami, Phys. Rev. B **42**, 5621 (1990).
[18] R. Shimano and M. Kuwata-Gonokami, Phys. Rev. Lett. **72**, 530 (1994).
[19] D. Fröhlich, P. Köhler, W. Nieswand, and E. Mohler, Phys. Status Solidi B **167**, 147 (1991).
[20] T. D. Lee, F. E. Low, and D. Pines, Phys. Rev. **90**, 297 (1953).
[21] O. Akimoto and E. Hanamura, J. Phys. Soc. Jpn. **33**, 1537 (1972).
[22] W. F. Brinkman, T. M. Rice, and B. Bell, Phys. Rev. B **8**, 1570 (1973).
[23] E. Tokunaga, A. L. Ivanov, S. V. Nair, and Y. Masumoto, Phys. Rev. B **63**, 233203 (2001).
[24] K. Saito, M. Hasuo, T. Hatano, and N. Nagasawa, Solid State Commun. **94**, 33 (1995).
[25] See Supplemetal Material at http://link.aps.org/supplemental/10.1103/PhysRevB.102.075203 for determined parameters, $A_{jk}^{(i)}$ and c_i, in the wave function of the biexciton.
[26] E. Tokunaga, K. Kurihara, M. Baba, Y. Masumoto, and M. Matsuoka, Phys. Rev. B **64**, 045209 (2001).
[27] T. Ando, M. Hasuo, and N. Nagasawa, Phys. Status Solidi B **179**, 453 (1993).
[28] T. Mita, K. Sôtome, and M. Ueta, Solid State Commun. **33**, 1135 (1980).
[29] S. V. Nair and T. Takagahara, Phys. Rev. B **55**, 5153 (1997).
[30] E. Hanamura, Solid State Commun. **12**, 951 (1973).
[31] A. L. Ivanov and H. Haug, Phys. Rev. B **48**, 1490 (1993).
[32] E. Tokunaga, A. L. Ivanov, S. V. Nair, and Y. Masumoto, Phys. Rev. B **59**, R7837 (1999).
[33] M. Born and E. Wolf, *Principles of Optics: Electromagnetic Theory of Propagation, Interference and Diffraction of Light*, 4th ed. (Pergamon Press, Oxford, 1969), Appendix V.